Colloids and Surfaces A 544 (2018) 86–90

Contents lists available at ScienceDirect

Colloids and Surfaces A

journal homepage: www.elsevier.com/locate/colsurfa

Effects of anisotropic liquid spreading on liquid transport in arrow-like micropillar arrays

Koji Muto, Daisuke Ishii*

Department of Life Science and Applied Chemistry, Graduate School of Engineering, Nagoya Institute of Technology, Nagoya, 466-8555, Japan

GRAPHICAL ABSTRACT

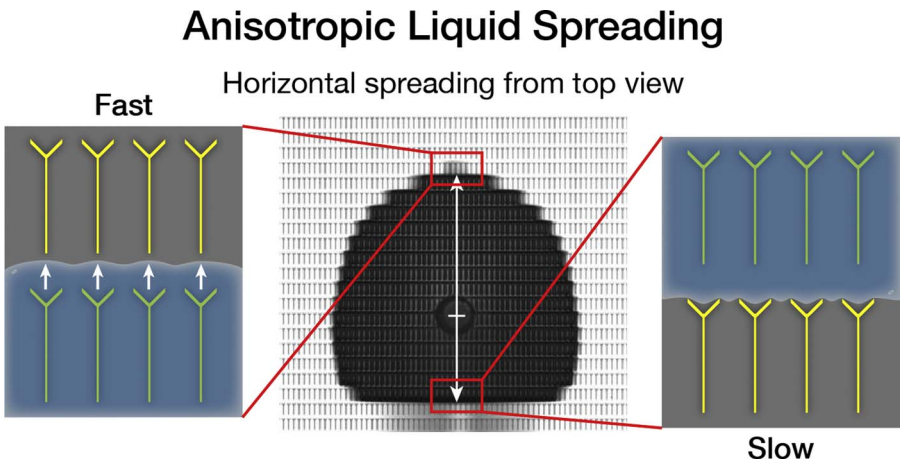

ARTICLE INFO

Keywords:
Wettability
Micropatterned surface
Arrow-like micropillar
Macroscale liquid transport
Microscale liquid spreading
Bioinspired

ABSTRACT

We investigated the acceleration and deceleration of wettability-driven liquid transport in arrow-like micropillar arrays. Arrow-shaped pillars were designed by combining a microplate-shaped pillar as a shaft, bioinspired by *Ligia exotica*, with an arrowhead shape. Micropatterned surfaces covered with arrow-like micropillars with a fixed height were conventionally designed and fabricated by lithography. After surface modification, the ability of the surfaces to transport water in the vertical direction from a pool was characterized using the Washburn equation. The design of the arrow-like pillar provided considerable acceleration or deceleration of liquid transport depending on the direction of the arrowhead of the pillar. We found the acceleration and deceleration of liquid transport on the patterned surfaces were derived from anisotropic liquid spreading on a microscopic scale.

1. Introduction

Manipulating liquids on micropatterned surfaces has a wide range of applications in microfluidic devices [1,2], anti-fouling surfaces [3,4], and heat pipes [5]. Recently, inspiration from smart surfaces in nature has prompted studies into micropatterned surfaces composed of asymmetric and anisotropic microstructures with unidirectional functionality induced by Laplace pressure gradients, including water droplet

* Corresponding author.
E-mail address: ishii.dasuke@nitech.ac.jp (D. Ishii).

https://doi.org/10.1016/j.colsurfa.2018.02.023
Received 17 November 2017; Received in revised form 31 January 2018; Accepted 10 February 2018
Available online 12 February 2018

spreading [6–9] and liquid transport on wettable surfaces [10,11]. Typical micropatterned surfaces composed of asymmetric and anisotropic microstructures, such as tilted pillars, pillars with a height gradient [12], and combinations of grooves and arc pits [13–15] are conventionally fabricated by photolithography through complex processes or using a negative mold fabricated by 3D printing [16]. However, submicrometer scale structures remain difficult to produce.

Feng et al. [17] reported unidirectional capillary-driven liquid transport in open structured surfaces composed of fin-decorated microgrooves with a fixed height. These surfaces exhibited strong pinning in the fin-tilting direction and rapid transport in the opposite direction. This unidirectional liquid transport occurs on micropatterned surfaces with fin-decorated microgrooves because the three-phase contact line (TCL) behavior at the transporting front is different from the liquid propagation mechanism, known as “zipping” [18–20], on micropatterned surfaces with micropillars. To induce unidirectional liquid transport in conventionally designed micropillar arrays with a fixed pillar height, anisotropic pillars such as triangular pillars [21–23] and pendant posts [24] are needed.

We previously reported a capillary-driven liquid transport system on anisotropic surfaces composed of microscale plate-shaped pillars mimicking those of *Ligia exotica* [25–29]. In this article, we describe the acceleration and deceleration of macroscale liquid transport on micropatterned surfaces caused by small changes in the pillar shape from plate- to arrow-like.

2. Methods

The micropatterned surfaces composed of microplate arrays and two types of arrow-like micropillar arrays were fabricated by photolithography. Negative photoresist (SU-8 3025, MicroChem, USA) was spin-coated on silicon wafers to form a 30-μm-thick film. The photoresist-coated wafers were then heated for 10 min at 95 °C, after which they were exposed to ultraviolet (UV) light through a photomask. The exposed samples were developed and then post baked for 10 min at 95 °C to provide micropatterned surfaces consisting of SU-8 pillars on the silicon wafer. The area of fabricated pillars was 25 mm (length) × 10 mm (width). The basic parameters of the pillars of length (slit length; *SL*), gaps (pitch interval; *PI* and line width; *LW*), height *h*, and thickness *w* were fixed at 100, 50, 50, 30, and 2 μm, respectively. The parameters of the arrowhead part illustrated in Fig. 1(a) including the breadth of the arrowhead *b*, distance from shaft *u*, length *v*, and gap between arrowheads *a* were 4, 15, 19, and 20 μm, respectively. The fabricated patterns of arrow-like pillars and directions of macroscale liquid transport are summarized in Fig. 1(b). An arrowhead is combined with the tip of each pillar. The liquid transport direction was determined by whether the arrowhead was parallel (top; $T^{\uparrow}$ and bottom; $B^{\uparrow}$) or antiparallel ($T^{\downarrow}$ and $B^{\downarrow}$) to the flow direction.

The prepared micropatterned surfaces were irradiated by vacuum UV/ozone treatment (500 ± 20 Pa, 20 min) to acquire a completely wetted state with water. The irradiated surfaces were placed in a dip coater and lowered toward a water pool. When the bottom surface made contact with the water pool, the water spontaneously started to be transported against gravity. The macroscale liquid transport behavior was recorded by a CCD camera (D5200, Nikon Corporation, Japan).

Microscale liquid spreading on the horizontal surfaces was measured using a contact angle goniometer (LSE-A110T, NiCK Corporation, Japan) that could record both top and side views. Each micropatterned surface was mounted on a stage, and then a small amount of water was extruded from a needle without suction so that no droplet formed to prevent the droplet mass affecting initial spreading. The micropatterned surface mounted on the stage was raised until it came into contact with the extruded water, whereupon the water spontaneously spread on the micropatterned surface. Liquid spreading experiments were also carried out using oil (silicone oil 10-cSt, Shin-Etsu Chemical) to compare spreading shape with water spreading. Spreading edges were recorded on a smaller scale using an optical microscope (VHX-2000, Keyence) to observe the wetting behavior around a pillar, which is related to the velocity of macroscale liquid transport.

3. Results

The contact angles of both water and silicone oil on an original silicon wafer and flat SU-8 surface after vacuum UV/ozone treatment were less than 10°. This indicates that vacuum UV/ozone treatment gave a sufficiently large surface energy to form a surface with homogeneous wettability. Transported water in each flow direction reached the end of micropatterned area (Fig. 2a and Movie S1 and S2). The velocities of macroscale liquid transport were analyzed by the Washburn equation [30], which stipulates that the position *z* of the TCL increases as the square root of time: $z = D\,t^{-2}$, where *D* is a coefficient [29]. Measured *D* values for each sample are displayed in Fig. 2b. The values of $T^{\uparrow}$ and $B^{\downarrow}$ are smaller than those of microplate arrays. Comparing the transport velocities of $T^{\uparrow}$ and $B^{\downarrow}$, $T^{\uparrow}$ is slightly higher than $B^{\downarrow}$. In the $T^{\downarrow}$ and $B^{\uparrow}$ flows, $T^{\downarrow}$ is considerably faster than $B^{\uparrow}$. These tendencies mean that including an arrowhead at the contacting point of the TCL makes it difficult for water to penetrate into the next row of dry pillars. Although the values of $T^{\downarrow}$ and $B^{\uparrow}$ cannot necessarily be compared with those of $T^{\uparrow}$, $B^{\downarrow}$, and microplate arrays because the gap length *PI* is shortened by the arrowhead protruding outside the shaft, the smaller values of $B^{\uparrow}$ than those of $B^{\downarrow}$ and microplate arrays suggest that an arrowhead protruding outside the shaft further inhibits the TCL from penetrating into the next dry region.

Fig. 3 shows the microscale water spreading behavior of the surfaces with different patterned arrays. Zipping behavior was observed at the

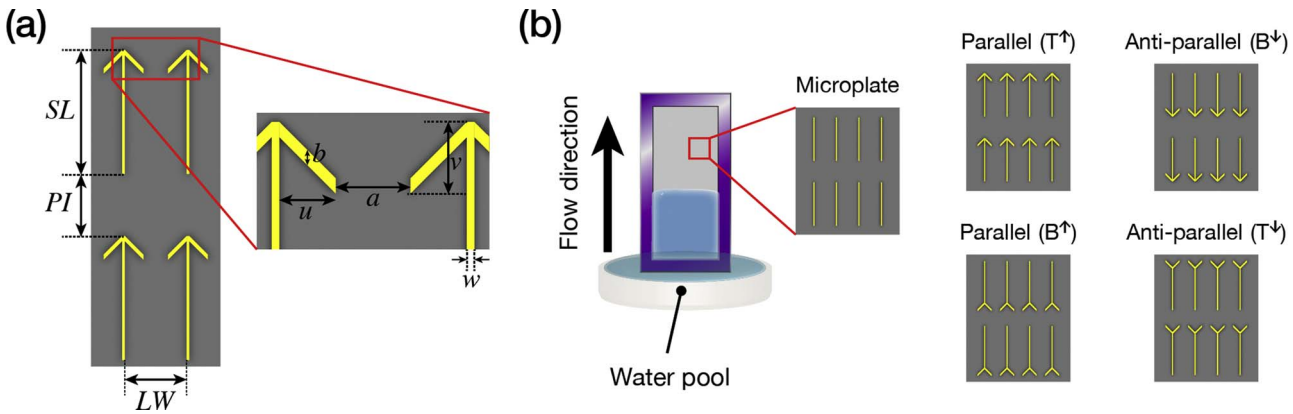

Fig. 1. (a) Parameters of micropatterned surfaces. (b) Schematic diagrams of macroscale liquid transport.